Characterization of optomechanical cavities

Author: Elisenda Vitrià Montero
*Facultat de Física, Universitat de Barcelona, Diagonal 645, 08028 Barcelona, Spain.**

Advisor: Daniel Navarro Urrios

Abstract: The coupling between optical and mechanical waves has been a growing study field for the last few years. Optomechanical crystals (OMCs), also known as Phoxonic crystals, are periodical nanostructures that can present bandgaps for both photons and phonons. By injecting a slight defect into the OMCs one can place particular modes inside the gaps enabling light and motion to effectively localize in the same volume, thus enhancing the optomechanical interaction. The latter allows the optical transduction of nanomechanical motion with near quantum-limited sensitivity, which drives us to applications such as signal processing and high-speed sensing systems. This study aims to experimentally characterize a set of optomechanical devices and point out their effectiveness in terms of their optical and mechanical quality factor (Q factor). In this regard, I have found that the best Q factor values appear as a compromise between the geometrical depth of the defect and the fabrication limitations, and I also noticed a significant difference between mechanical and optical losses due to their main dissipating mechanisms, leading to lower mechanical Q factors.

I. INTRODUCTION

Cavity optomechanics is defined as the research field that studies the interaction between electromagnetic radiation and micro or nano-mechanical motion inside an optical cavity. Its name relates to the principal effect, which is to increase the radiation pressure and matter interaction through optical resonators (commonly called *cavities*). Within this decade, this field has been on a constant rise, achieving excellent progress and leading to great applications in communications and sensing.

The so-called OMCs are nano-patterned metamaterials or dielectrics fabricated to control and manipulate the propagation of light and sound. They combine the properties of both photonic and phononic crystals, designed to confine optical and mechanical modes, respectively, and form a complete optomechanical system (Ref. 1).

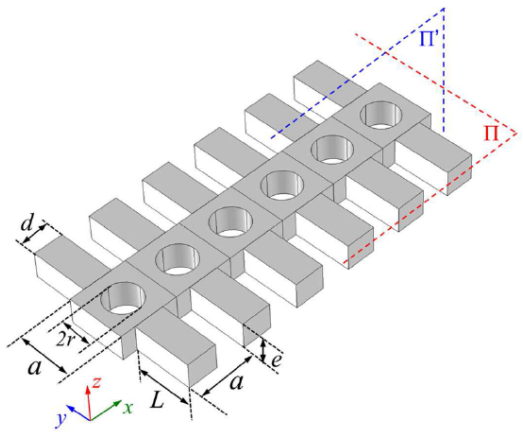

FIG. 1: OMC with its symmetry planes (Π and Π′) and geometry parameters (a, L, d, r and e). See Ref. 2.

*Electronic address: e.vitria6@gmail.com

This paper is organized into four sections as follows. In the first section, an introduction about the structure implemented and its particular design. In the second section, a brief explanation of the laboratory setup where the experiment has taken place. In the third section, the main discussion involving the Q factor and how to compute it, concluding with the fourth section, estimating the most efficient structure among the given samples.

Previous work has concluded that a particular 1D silicon OMC exhibits bandgaps for electromagnetic (in the hundreds of THz) and mechanical (in the GHz) waves. It consists of a straight silicon nanobeam waveguide with parallelepiped stubs attached on both sides and circular holes drilled in the middle, as illustrated in Fig.(1). It provides an absolute phononic bandgap and a photonic bandgap for TE-like (Transverse Electric) optical modes (Ref. 3).

Furthermore, it was realized that adding a defect, also called a *phoxonic cavity*, into these crystals leads to high Q factors, which are crucial to obtain a better coupling and improve their applicability. This cavity is formed by gradually reducing the unit cell parameters with the same percentage (Γ) with respect to the original values: the cell width (a), stub width (d), and hole radius (r) from both sides of the waveguide towards the center, leaving the thickness (e) as a constant along the structure, since it is determined by the silicon layer thickness. Hence, the middle cells are smaller than the normal ones, the latter thus acting as mirrors located on both sides. The main advantage of this structure resides in the fact that now this cavity will be able to confine particular photonic and phononic modes inside the gaps enabling the enhancement of the optomechanical interaction and increasing the Q factor of the trapped light. As I pointed out before, the side cells will act as mirrors, meaning that the modes placed inside the gaps won't exist in their spatial domain, and thus it will confine them even more, avoiding leakage.

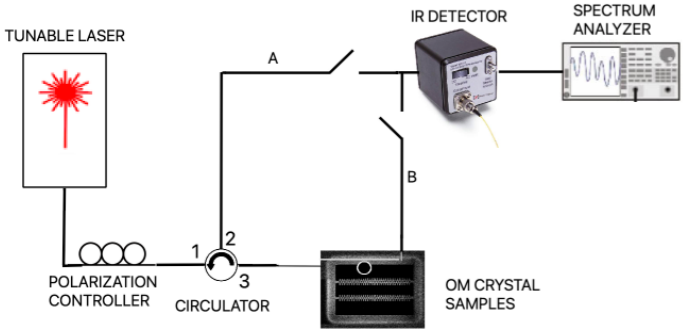

FIG. 2: Experimental setup diagram. After reaching the polarization controller, light enters the OMC cavity exciting a particular optical mode that couples with the mechanical modes. The IR detector collects the reflection or transmission signal from both directions of the fiber, path A or B in the figure, to probe the optical resonator. Then via the spectrum analyzer, I identified the mechanical modes confined in the cavity and enhanced by the coupling.

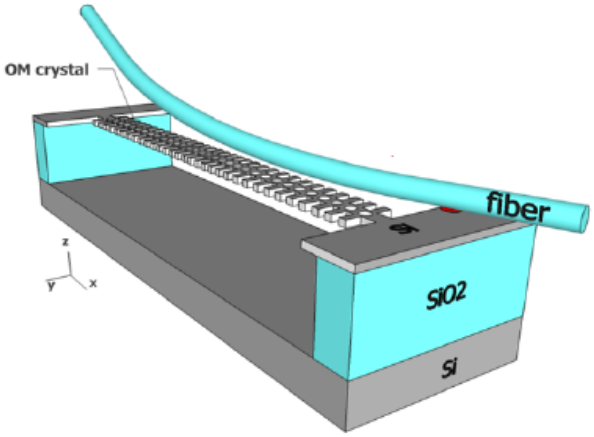

FIG. 3: Fiber placed into the near field of the OMC cavity.

II. LABORATORY SETUP

The experiment performed aims to analyze a set of OMCs with different properties. The samples were built using e-beam lithography, a technique to create small structures by the scanning of a focused energetic beam of electrons on a resist. In order to find optimum fabrication conditions, different sets of nominally equivalent structures have been fabricated where the e-beam dose has been changed. In other words, the nano-patterned structures are slightly different when it comes to size and shape. Moreover, each group of structures fabricated with the same e-beam dose includes five of them with Γ parameters ranging from 1 to 0.80, and two identical structures per gamma value separated 2 μm (see Fig.2).

Measurements were taken for one batch with the same dose since I observed that the structures fabricated with larger and lower doses were not displaying optical modes within the spectral range of our tunable laser. It is worthwhile noticing that structures with $\Gamma = 1$ were not taken into account. Since there are no reduced cells, no cavity has been created in these OMCs.

The experimental setup, illustrated in Fig.(2), has the following course. First, a tunable laser, in which one can vary the power and wavelength of the light injected in the cavity, ranging from 1470 nm to 1590 nm. Afterwards, the light propagating through the fiber reaches a polarization controller. Achieving a good coupling requires the maximum power to arrive at the cavity, and therefore, light polarization has to be aligned with the polarization of the supported cavity modes, which in the case under study is TE (the electric field oscillating along the y-direction). In order to effectively probe these microphotonic devices, I used a technique that utilizes a tapered optical fiber, heated and stretched down to a diameter on the order of a micron, in which a tens of microns diameter loop has been made. Due to the small diameter of the fiber, only one mode will propagate through it, meaning that part of the electromagnetic wave will propagate outside the limits of the fiber material, forming an evanescent wave (Ref. 1). Light enters the OMC cavity and excites a particular optical mode that couples with the mechanical modes. I used an IR detector to receive the signal arriving from the fiber. The input can be from two different sources, path A or B in Fig.(2). Path A carries the reflection signal, as the 2nd output of the circulator collects the resonant modes coming from the 3rd output that entered the cavity and were reflected by it. Path B conveys the transmitted signal, namely, the rest of the wavelengths. Finally, the signal reaches the spectrum analyzer. Its primary use is measuring the radiofrequency (RF) power spectrum of the input signal. By setting the laser wavelength within the optical resonance, I could extract the noise frequency spectrum embedded in the transmission signal and its magnitude, more precisely, the mechanical modes coupled with that optical mode and modulating its natural position. The latter is caused by the *transduction mechanism*, as explained hereafter in this document.

III. OPTICAL AND MECHANICAL Q-FACTOR

In terms of optical resonance, the Q factor is a dimensionless parameter that gives a measure of the damping of resonator modes. It can be determined by calculating how many times a wave trapped within the cavity will bounce before escaping. Also, it is defined as the ratio of the resonance wavelength (λ_0) to its full width at half-maximum ($\Delta\lambda$). Equating these last two definitions leaves the following expression:

$$Q_{tot} = w_0\tau = \frac{2\pi\tau}{T} = \frac{\lambda_0}{\Delta\lambda} \tag{1}$$

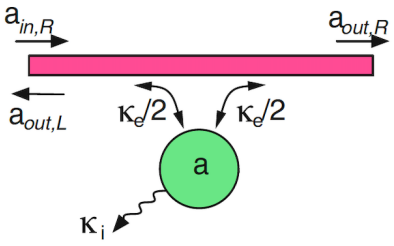

FIG. 4: Double sided coupling cavity (a), seen in Ref. 1, with its intrinsic loss rate (k_i) and extrinsic loss rate (k_e) parameters.

, where w_0 is the resonance frequency, τ the lifetime of the photons inside the cavity, and T the mode's oscillations period.

In order to evaluate the Q factor of the particular cavity studied in this document, it is appropriate to look into the parameters involved using a simple model. Fig.(4) presents the so-called double-sided coupling cavity. Its primary characteristic is that light can escape into both directions of the fiber, the transmitted field goes into the forward channel ($a_{out,R}$), and reflection goes into the backward channel ($a_{out,L}$). The total optical energy decay rate is a magnitude related to the lifetime of the photons as $k = \tau^{-1}$ and used to evaluate the losses of the loaded cavity:

$$k = 2\left(\frac{k_e}{2}\right) + k_i \tag{2}$$

The contribution k_i is known as the *intrinsic loss rate*, referring to the loss of the system due to surface/volume scattering and/or material absorption. The *extrinsic loss rate* (k_e) is associated to the additional optical loss channel associated to the presence of the fiber. Finally, from joining Eq.(1) and Eq.(2) arises the expression to sum the two contributions of the Q factor:

$$\frac{1}{Q_{tot}} = \frac{1}{Q_e} + \frac{1}{Q_i} \tag{3}$$

Moreover, it is convenient to use the transmitted field collected by the channels, whereby I extracted the optical parameters to determine Q_{tot} and Q_e. The transmission has the following expression (Ref. 1):

$$T = \left|\frac{a_{out}}{a_{in}}\right|^2 = \left|1 - \frac{\eta k}{i\Delta + k/2}\right|^2 \tag{4}$$

, where $\Delta = w_0 - w_{laser}$ and $\eta = 2k_e/k$, which is called *coupling efficiency*. One can notice that for perfect resonance $\Delta = 0$, and thus the transmission will be:

$$T = T_0 = (1-2\eta)^2 = \left(1 - \frac{k_e}{k}\right)^2 \tag{5}$$

The *transmission depth* (T_0) is obtained by dividing the power transmitted with perfect resonance by the power arriving when the light is not coupled.

As stated in the Laboratory Setup section, the connection between the optical Q and the observation of mechanical modes is exemplified with the transduction mechanism in Fig.(5). The effect is caused by the coupling between light and mechanical waves. The mechanical motion moves the photonic cavity resonance at the mechanical eigenfrequencies, inducing the modulation of the transmitted signal. Hence the amplitude of this wave heavily depends on the slope of the resonance, namely the value of the optical Q factor. If the latter is high, the modulation amplitude will increase, and the mechanical modes composing it will stand out from the noise.
It must be stressed that all the mechanical modes already exist inside the cavity, but I only detected those that are strongly coupled to the optical mode and are populated thermally.

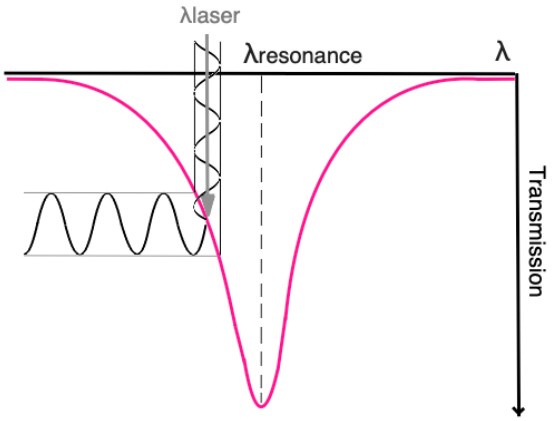

FIG. 5: Simple representation of the transduction mechanism, in which the optical resonance's position is modified by mechanical motion and induces the modulation of the transmission.

A. Optical Modes

Regarding this subsection, the primary purpose is to investigate the photonic TE modes placed into the gap that achieve a high Q factor while confined inside the cavity. From Fig. (6), we can see both reflection and transmission at low optical input power ($\sim 0.2mW$), highlighting the concordance of the resonance positions for the two signals. It is noted that the collected transmission spectrum exhibits some ripples in between resonance wavelengths, which correspond to modes that originated inside the loop of the fiber through constructive and destructive conditions, forming an unwanted cavity. Consequently, I evaluated the total Q factor using the reflected signal.
For simplicity, I used the fundamental mode displayed

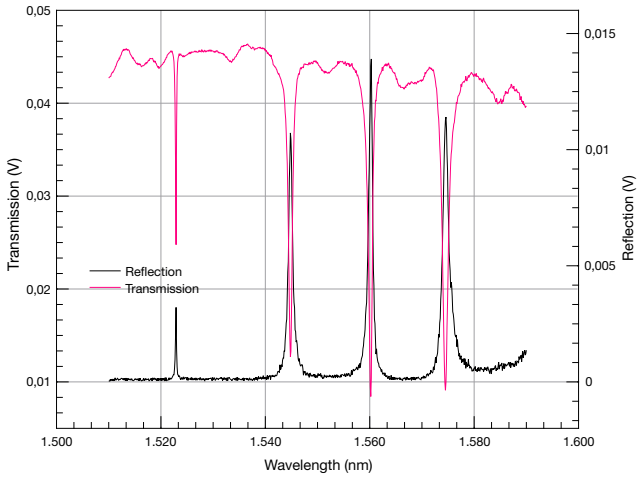

FIG. 6: Detected optical signal from reflection and transmission channels displaying the first modes for a $\Gamma = 0.85$ cavity.

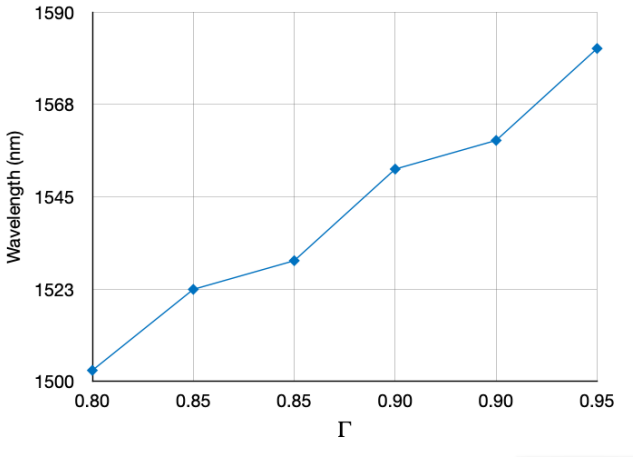

FIG. 8: Cavities with their corresponding fundamental mode's wavelength.

by each OMC to make the calculations. Data analysis was performed by OriginLab, determining λ_0 and $\Delta\lambda$. Also, using Eq. (1),(3), and (5) I extracted the values for Q_{tot}, Q_e, and Q_i. Fig. (7) shows the evolution of the two contributions and the total Q factor through all six OMCs.

With an overall view of the parameters found, one can characterize the optical properties of the OMCs. From Fig. (8) we can observe that by increasing the tapering of the defect, the wavelength of the photonic mode shifts towards longer wavelengths, while the intrinsic Q factor finds a maximum in the OMCs with Γ=0.85 and 0.9. The former behavior occurs due to the change in the effective optical index at the center of the defect, which is higher at narrow cavities, allowing modes with higher frequencies to confine.

B. Mechanical Modes

As mentioned previously, once the signal is fixed within any optical resonance, it is possible to feature the existing mechanical modes that are thermally activated and have enough optomechanical coupling to overcome the noise level. I obtained the total spectrum of each OMC at high input power ($\sim 4mW$), where I could see two separated ranges of frequencies, as shown in Fig. (9). Firstly, low-frequency modes ($\sim 0 - 100MHz$) that correspond to flexural modes of the nanobeam. Even though the structures were not designed to display coupling for these phonons, they have proven to display a high Q factor. That can be explained due to the interaction between the electromagnetic field asymmetry and the vibrating structure distribution at that frequency, giving rise to a high coupling between them, as reported in Ref. 4. I

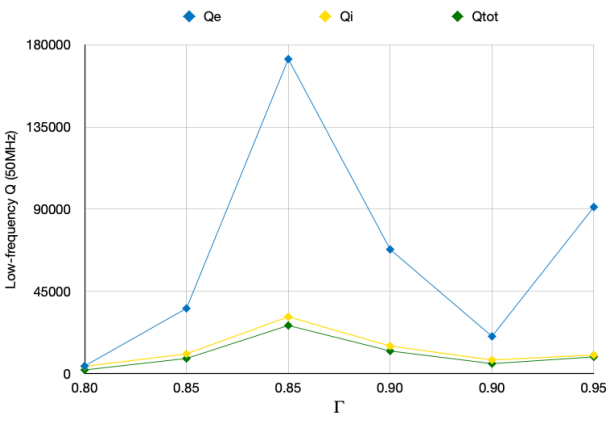

FIG. 7: Estimated intrinsic, extrinsic and total optical quality factor of the OMCs.

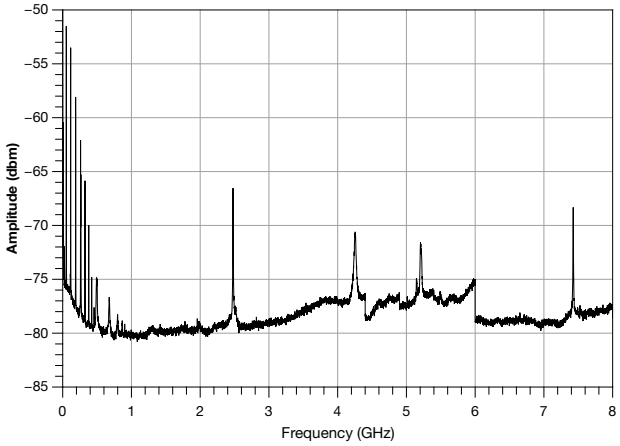

FIG. 9: Detected frequency spectrum displaying the enhanced mechanical modes inside the cavity.

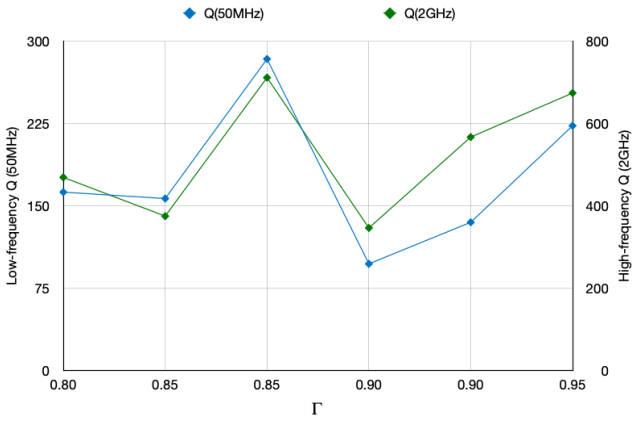

FIG. 10: Estimated low-frequency ($50MHz$) and high-frequency ($2.4GHz$) mechanical mode's quality factor of the OMCs.

took the $50MHz$ mode as a reference, a flexural in-plane mode with three anti-nodes.

Analyzing Fig. (10), we can notice low Q factors for the $50MHz$ mode due to its dominant dissipating mechanism, which is associated with room atmospheric conditions, inducing most of the losses for this type of phonons. Secondly, high-frequency modes ($\sim 1-8GHz$) referring to localized breathing modes of the structure. When it comes to a suitable coupling of localized photons and phonons, the mode's symmetry plays an important role. So, for any optical field, the coupling only occurs if the phononic wave displays an even symmetry field distribution with respect to both Π'(XZ) and Π(XY) planes of the nanobeam. As reported by Gomis et al. [4], the band structure shows three pseudo-gaps for EE phononic modes within which we can find two localized states with this very symmetry at $5.2GHz$ ($Q_{mec} = 1200$) and $7.4GHz$ ($Q_{mec} = 2200$). Since they are placed inside a pseudo-gap, there is no interaction between them and other modes with different symmetries (as long as they can stay orthogonal), thereby providing a fairly high Q factor. Furthermore, given that the $5.2GHz$ and $7.4GHz$ modes have a low OM coupling, I could only see them displayed by the better OMCs.

It is worth noticing that there is also a resonant phonon mode around $2.4GHz$. Unlike the other states, this one is created outside any bandgap, interacting with its own original band on the mirror regions, as we can see in Ref. 2, and leading to a poor Q factor compared to the other high-frequency modes. Nonetheless, given that the crossing point is located at a relatively high wavenumber, there is no significant leakage through the mirrors, and the state is still well confined.

IV. CONCLUSIONS

In sum, this work intended to point out which OMC presented the most effective cavity to study light-matter interaction in a set of OMCs fabricated with different e-beam doses and geometrical parameters. The two main conclusions that can be extracted are the following:

- Regarding the optical Q factor, we can easily see the strong dependence between Q_i and Q_{tot}. As the intrinsic loss alludes to imperfections and manufacturing defects, it becomes more relevant to the total Q factor than the extrinsic loss, mostly caused by the positioning of the fiber. Besides, from Fig. (7), we can note that the 3rd sample ($\Gamma = 0.85$) presents the highest Qi value for the three contributions, leading us to believe that it has the most accurate design and fabrication.

- Also, the 3rd OMC remains the most effective cavity presenting the greater values for both mechanical modes. Nominally there is no direct relation between the optical and mechanical Q factor. However, considering that the cavity fabricated with fewer imperfections can improve the confinement of phonons and photons, it is likely to find a similar evolution of these values through all OMCs.

Acknowledgments

First, I would like to express my gratitude to my advisor for his practical advice, engaging lessons, and endless patience during the experimental sessions. I also wish to express my thanks to the University of Barcelona for providing such an equipped laboratory to conduct my study. Finally, to my friends and family, whose motivation and support helped me carry on this project.

[1] Aspelmeyer, Markus, Tobias J. Kippenberg, and Florian Marquardt. "Cavity optomechanics." Reviews of Modern Physics 86.4 (2014): 1391.

[2] Oudich, Mourad, et al. "Optomechanic interaction in a corrugated phoxonic nanobeam cavity." Physical Review B 89.24 (2014): 245122.

[3] Gomis-Bresco, Jordi, et al. "A one-dimensional optomechanical crystal with a complete phononic band gap." Nature communications 5.1 (2014): 1-6.

[4] Navarro-Urrios, Daniel, et al. "A self-stabilized coherent phonon source driven by optical forces." Scientific reports 5.1 (2015): 1-7.